Materials Transactions, Vol. 45, No. 7 (2004) pp. 2137 to 2143
Special Issue on Grain Boundaries, Interfaces, Defects and Localized Quantum Structures in Ceramics

Atomic and Electronic Structures of Ni/YSZ(111) Interface

Takeo Sasaki[1,*], Katsuyuki Matsunaga[2], Hiromichi Ohta[3], Hideo Hosono[3], Takahisa Yamamoto[4] and Yuichi Ikuhara[2]

[1]*Department of Materials Engineering, School of Engineering, The University of Tokyo, Tokyo 113-8656, Japan*
[2]*Institute of Engineering Innovation, The University of Tokyo, Tokyo 113-8656, Japan*
[3]*Hosono Transparent ElectroActive Materials, ERATO, Japan Science and Technology Corporation, Kawasaki 213-0012, Japan*
[4]*Department of Advanced Materials Science, The University of Tokyo, Tokyo 113-8656, Japan*

Thin Ni films were deposited on the (111) surface of YSZ at 1073 K by a pulsed laser deposition technique. The interfacial atomic structure of Ni/YSZ was investigated by high-resolution transmission electron microscopy (HRTEM). It was found that Ni was epitaxially oriented to the YSZ surface, and the following orientation relationship (OR) was observed: $(111)_{Ni} \parallel (111)_{YSZ}$, $[1\bar{1}0]_{Ni} \parallel [1\bar{1}0]_{YSZ}$. Geometrical coherency of the Ni/YSZ system was also evaluated by the coincidence of reciprocal lattice points (CRLP) method. It was found that the most coherent OR predicted by CRLP method was $(705)_{Ni} \parallel (111)_{YSZ}$, $[0\bar{1}0]_{Ni} \parallel [1\bar{1}0]_{YSZ}$, which was not consistent with the experimentally observed OR. To understand the detailed atomic structure, HRTEM image simulations were performed. However, simulated images based on both O-terminated and Zr-terminated interface models were quite similar to the experimental image, and thus it was hard to determine which model is comparable with the actual interface only by the HRTEM image simulations. In order to clarify the termination layer at the interface, electronic structures of the Ni/YSZ interface were investigated by electron energy-loss spectroscopy. It was found that significant differences were observed in O-K edge spectra between the interface and the YSZ crystal interior, and the spectrum from the interface showed similar features to the reference spectrum of bulk NiO. This indicates that the Ni-O interaction occurs at the interface to terminate the oxygen {111} plane of YSZ at the Ni/YSZ interface. In addition, the density of Ni-O bonds across the interface in the experimental OR was larger than that in the most coherent OR predicted by CRLP method, which also suggests that the on-top Ni-O bonds stabilize the Ni/YSZ(111) interface.

(Received January 30, 2004; Accepted March 11, 2004)

Keywords: *nickel/yttria-stabilized zirconia interface, atomic structure, electronic structure, high-resolution transmission electron microscopy, electron energy-loss spectroscopy, coincidence of reciprocal lattice points method*

1. Introduction

Metal-ceramic interfaces play an important role for performance of advanced materials such as thermal barrier coatings (TBCs), solid oxide fuel cells (SOFCs), composites, electronic packaging devices and catalytic materials. As a typical example, metal-ceramic interfaces in TBCs used in turbine engines for power generation are subjected to severe ambiences such as high temperatures and corrosive atmosphere. In the TBC system, yttria-stabilized zirconia (YSZ) films are usually deposited on Ni-based metallic substrates, which protect the metallic substrates from thermal degradation due to low thermal conductivity of YSZ. During high-temperature operation of the TBC system, however, it was often observed that thermally grown oxides such as Al_2O_3 are formed at the YSZ-metal interfaces, and subsequently cracking and delamination also take place.[1,2)]

On the other hand, NiO-YSZ and Ni-YSZ cermets are utilized as anode materials in the SOFC system. In this case, the metal-ceramic interfaces are also subjected at high temperatures and reduction atmosphere, which cause a coarsening of reduced Ni grains. The coarsening has been reported to decrease the number of the three-phase boundary such as a Ni/YSZ/fuel gas, which is essential for catalytic activity, finally giving rise to degradation of electric properties.[3,4)] Since these phenomena are closely related to physical and chemical properties of the Ni/YSZ interfaces, it is important to obtain fundamental understanding of atomic and electronic structures at the Ni/YSZ interface in detail.

Recently, several theoretical studies based on ab initio calculations have been performed for Ni-ZrO_2 interfaces. Christensen and Carter reported that the O-terminated interface is energetically favorable in the $ZrO_2(111)$/Ni(111) interface.[5)] Han *et al.* reported that the Ni-O interaction plays an important role for the adhesion of the Ni(001)/ZrO_2(001) and Ni(111)/ZrO_2(111) interfaces.[6,7)] On the other hand, Beltrán *et al.* reported that both the Zr-terminated and O-terminated interfaces are energetically favorable in the Ni(001)/ZrO_2(001) interface.[8,9)] In addition to the theoretical studies, several experimental studies have been carried out. Dickey *et al.* studied the Ni/ZrO_2 interfaces, using Z-contrast imaging technique and EELS analysis, which were fabricated by reduction of the eutectic bonded NiO/ZrO_2 interface, and pointed out that the metallic bonding between Ni and Zr, which may be formed under the reduced atmosphere, is responsible for the stability of the Ni(111)/ZrO_2(001) interface.[10)] Dickey *et al.* also studied Ni/YSZ interface fabricated by molecular beam epitaxy, using electron diffraction technique, and found the predominant orientation relationship (OR) of $(111)_{Ni} \parallel (100)_{YSZ}$ and $[\bar{1}10]_{Ni} \parallel [010]_{YSZ}$, and the minor cube-on-cube OR of $(100)_{Ni} \parallel (100)_{YSZ}$ and $[010]_{Ni} \parallel [010]_{YSZ}$.[11)] They investigated both the predominant and minor ORs from a geometrical perspective using near coincidence site lattice (NCSL) theory,[12,13)] and the results showed that the predominant OR was successfully rationalized but the minor OR was not able to be rationalized. They pointed out that theoretical calculations are necessary in order to clarify the origin of the minor OR. Although several theoretical and experimental studies have been performed for Ni/YSZ interfaces, not only the preferred OR but also the atomic structure and the energetically favorable termination in the Ni/YSZ interface have not been well understood. It is,

*Graduate Student, The University of Tokyo

therefore, important to understand the atomic and electronic structure as well as the preferred OR in the Ni/YSZ interface.

In this study, atomic structure of Ni/YSZ(111) interface fabricated by a pulsed-laser deposition (PLD) technique was characterized by high-resolution transmission electron microscopy (HRTEM). The electronic structure of Ni/YSZ(111) interface was analyzed by electron energy-loss spectroscopy (EELS). In addition, the preferred OR of the Ni/YSZ interface was investigated by the coincidence of reciprocal lattice points (CRLP) method[14] and the origin of the observed OR of the Ni/YSZ interfaces was discussed.

2. Experimental Procedure

Ni metal with 99.99% purity (Kojundo Chemical Laboratory Co., Ltd) was used for deposition on the (111) surface of YSZ (ZrO_2-9.6 mol% Y_2O_3) (Shinkosha Co., Ltd) by PLD. The YSZ substrate was heated at 1073 K during deposition, and the pressure in the chamber was set to 10^{-6} Pa just before deposition. A KrF excimer laser beam (wavelength = 248 nm, pulse duration = 20 ns, repetition frequency = 20 Hz) was focused onto a rotating Ni target to produce a photon power density of about 2 J/cm^2/pulse. Then Ni metal was deposited by a deposition rate of 1 nm/min. Subsequently, thin foils for HRTEM observations were prepared by a standard procedure involving mechanical grinding to a thickness of 15 μm and additional Ar^+-ion beam thinning at an accelerating voltage of about 4.5 kV. The interfacial atomic structures of the fabricated samples were investigated by HRTEM using a JEOL JEM-4010 operated at 400 kV. Geometrical coherency between Ni and YSZ crystals was calculated by CRLP method in order to examine preferred ORs between the two crystals and make comparison with the experimentally observed OR. The experimentally obtained images were analyzed by comparison with simulated images based on possible structural models using the multislice method.[15] In order to reveal chemical bonding states at the interface, EELS measurements were carried out with a probe size of less than 1.5 nm, using a GATAN ENFINA spectrometer (energy resolution of 1.2 eV) attached to a TOPCON EM-002BF field emission TEM at the accelerating voltage of 200 kV.

3. Results and Discussion

3.1 HRTEM Observation

Conventional-TEM observations of the fabricated samples showed that Ni exhibits an island-like shape on the YSZ substrate and each island has about 30 nm in thickness. Figure 1 shows the cross-sectional HRTEM image of the Ni/YSZ(111) interface, where an incident beam direction was parallel to the $[1\bar{1}0]$ direction of YSZ. It should be noted that the HRTEM images were systematically taken at defocus values from 0 to −80 nm at an interval of about 10 nm. The interface was atomically flat, and no amorphous phase was observed. In addition, it was found that the Ni(111) plane was epitaxially orientated to the YSZ(111) surface in the following cube-on-cube OR,

$$(111)_{Ni} \parallel (111)_{YSZ}, \quad [1\bar{1}0]_{Ni} \parallel [1\bar{1}0]_{YSZ}. \qquad \text{OR (I)}$$

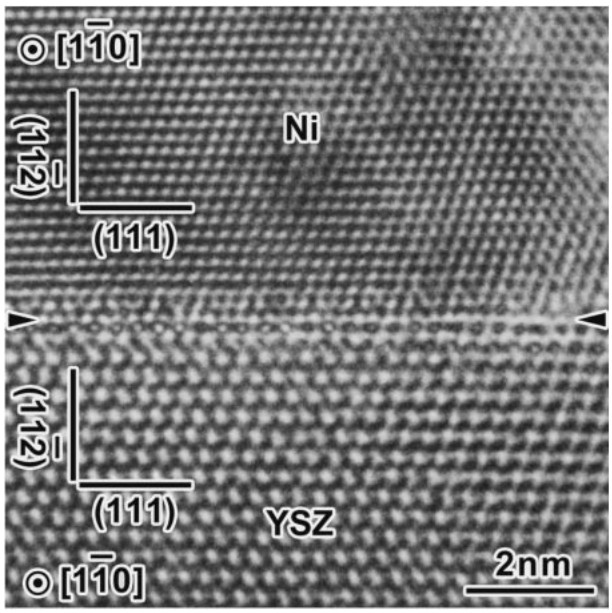

Fig. 1 HRTEM image of the Ni/YSZ(111) interface. The Ni(111) plane is epitaxially orientated to the YSZ(111) surface and the cube-on-cube OR is formed.

In this OR (I), a misfit parameter δ between Ni and YSZ crystals parallel to the interface plane is defined as

$$\delta_{Ni[11\bar{2}]/YSZ[11\bar{2}]} = \frac{|d_{(11\bar{2})Ni} - d_{(11\bar{2})YSZ}|}{d_{(11\bar{2})YSZ}} = \frac{|a_{Ni} - a_{YSZ}|}{a_{YSZ}} = 31\% \qquad (1)$$

where "d" and "a" are interplanar spacings and lattice parameters ($a_{Ni} = 0.352$ nm, $a_{YSZ} = 0.514$ nm), respectively. Because of the large misfit, the interface is expected to be an incoherent interface. In fact, no misfit dislocations accommodating the lattice misfit were observed. It can be said that the incoherent interface was formed in the interface. Similar incoherent interfaces were observed in other metal-ceramic interfaces such as Cu/Al_2O_3 interfaces.[16,17] In general, these incoherent interfaces have weak interactions across the interface. In order to clarify the origin of the weak interactions, it is necessary to investigate the preferred OR and the atomic structure.

3.2 Geometrical Coherency

In order to evaluate the preferred ORs for the Ni/YSZ(111) interface, the ORs with geometrically high coherency between two crystals were calculated by CRLP method. In the previous study by Ikuhara and Pirouz, the CRLP calculation was applied to V/Al_2O_3 interfaces,[18,19] and the calculated OR with highest coherency was found to be consistent with the experimental one.[20,21] Therefore, this calculation may be able to predict the most coherent OR between two different crystals. In this method, the overlap of reciprocal lattice points of two adjoining crystals was considered in order to obtain the geometrically optimum OR between the two crystals. Assuming reciprocal lattice points as spheres with finite volumes, the geometrical

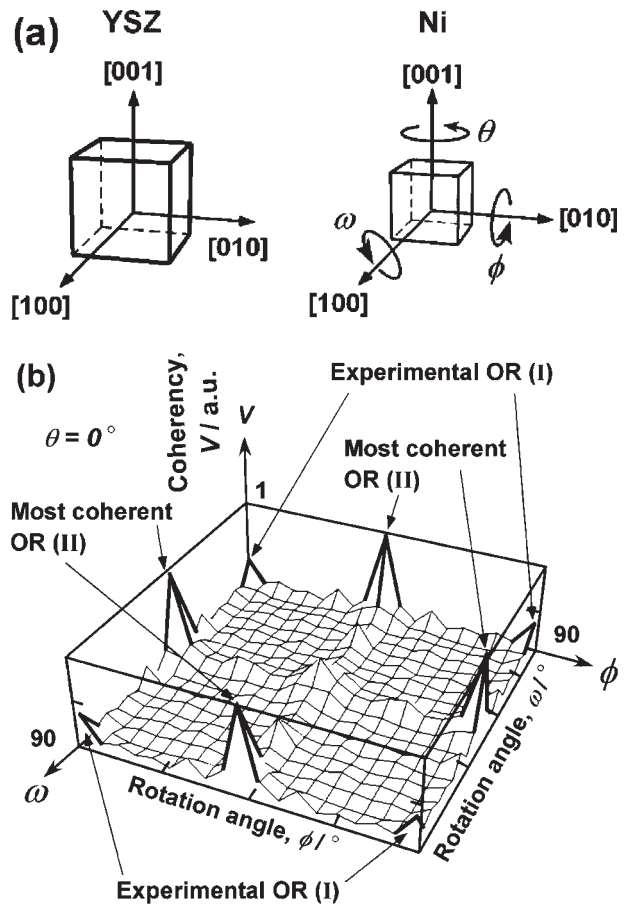

Fig. 2 (a) Schematic illustration of the initial OR for CRLP calculation. (b) Geometrical coherency at the rotation angle $\theta = 0°$ calculated by CRLP method. The longitudinal axis represents geometrical coherency V, whereas each horizontal axis represents the rotation angles ω and ϕ, respectively.

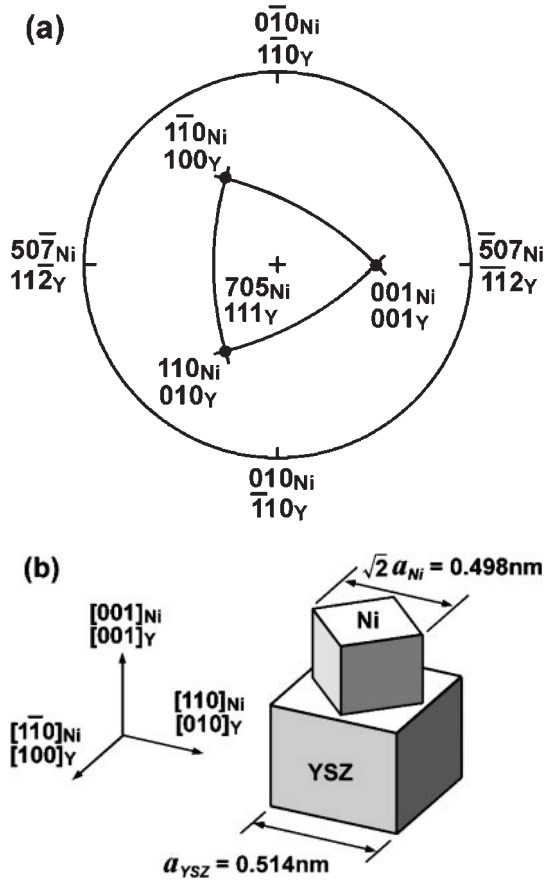

Fig. 3 (a) Stereographic projection of the Ni and YSZ crystals in the most coherent OR (II), where YSZ is denoted as Y. In this OR, it can be seen that Ni(001) and YSZ(001), and Ni(110) and YSZ(010) are parallel to each other, respectively, as well as Ni(705) and YSZ(111). (b) Schematic illustration of the most coherent OR (III), where YSZ is denoted as Y.

coherency was evaluated by summing the overlapped volumes of the reciprocal lattice spheres of two crystals, when one crystal was rotated three-dimensionally with respect to another. The sum of all overlapped volumes represents degrees of the parallelism and the coincidence of the spacings between the two lattices across the interface.

In the present case, the radii of reciprocal lattice spheres were taken to be 0.15 times as long as the length of the primitive reciprocal vectors of each crystal so that these reciprocal lattice spheres can overlap with one another (See Ref. 14). At the beginning of calculations, the (100), (010) and (001) plane of both Ni and YSZ were initially set parallel, as shown in Fig. 2(a). This initial OR is equivalent to the experimental OR (I) because of the cube-on-cube OR. Total overlapped volumes of reciprocal lattice spheres of Ni and YSZ were calculated by rotating Ni crystal three-dimensionally around [100], [010] and [001] axes, where rotation angles around [100], [010] and [001] axes were defined as ω, ϕ, θ, respectively.

Figure 2(b) shows the variation of geometrical coherency V against the rotation angles ω and ϕ at $\theta = 0°$. It is noted here that the CRLP calculations were performed by changing θ values from 0° to 90° in this study. However, most coherent peaks were confirmed to appear at $\theta = 0°$. For simplicity, therefore, only the result at $\theta = 0°$ is displayed in Fig. 2(b). It can be seen that the most prominent peaks are present at $(\omega, \phi, \theta) = (0°, 45°, 0°)$, $(45°, 0°, 0°)$, $(45°, 90°, 0°)$ and $(90°, 45°, 0°)$. These four sets of rotation angles are equivalent to each other, and represent the following OR with respect to the (111) plane of YSZ,

$$(705)_{\mathrm{Ni}} \parallel (111)_{\mathrm{YSZ}}, \quad [0\bar{1}0]_{\mathrm{Ni}} \parallel [1\bar{1}0]_{\mathrm{YSZ}}. \qquad \text{OR (II)}$$

Although the oriented plane of Ni is a high index plane, this OR can be confirmed to be high coherency in a stereographic projection. Figure 3(a) shows the stereographic projection of the Ni and YSZ crystals in the most coherent OR (II), where YSZ is denoted as Y. In this OR, it can be seen that Ni(001) and YSZ(001), and Ni(110) and YSZ(010) are parallel to each other, respectively, as well as Ni(705) and YSZ(111). Therefore, the OR (II) can be represented for the YSZ{001} in the following manner, as shown in Fig. 3(b),

$$(001)_{\mathrm{Ni}} \parallel (001)_{\mathrm{YSZ}}, \quad [110]_{\mathrm{Ni}} \parallel [010]_{\mathrm{YSZ}} \qquad \text{OR (III)}$$

$$(110)_{\mathrm{Ni}} \parallel (010)_{\mathrm{YSZ}}, \quad [001]_{\mathrm{Ni}} \parallel [001]_{\mathrm{YSZ}} \qquad \text{OR (III)}$$

where the OR (III) is equivalent to the OR (II). In case of the OR (III), a misfit parameter along the direction of $[110]_{\mathrm{Ni}}$ and $[010]_{\mathrm{YSZ}}$ is defined as

$$\delta_{\mathrm{Ni}[110]/\mathrm{YSZ}[100]} = \frac{|2d_{(110)\mathrm{Ni}} - d_{(010)\mathrm{YSZ}}|}{d_{(110)\mathrm{YSZ}}}$$

$$= \frac{|\sqrt{2}a_{\mathrm{Ni}} - a_{\mathrm{YSZ}}|}{a_{\mathrm{YSZ}}} = 3\% \qquad (2)$$

It is considered that this small misfit causes the largest total overlapped volumes and the most coherent OR.

On the other hand, it can be seen that small peaks are present at $(\omega, \phi, \theta) = (0°, 0°, 0°)$, $(0°, 90°, 0°)$, $(90°, 0°, 0°)$ and $(90°, 90°, 0°)$ in Fig. 2(b). These four sets of rotation angles, which are also equivalent to each other, correspond to the experimental OR (I). Although this OR has the second highest coherency, the highest coherent OR (II) predicted by the CRLP calculation is not consistent with the OR (I). It can be said that the experimental OR in the present Ni/YSZ(111) interface cannot be understood only from the geometrical coherency between the two crystals. This indicates that detailed atomic structures and chemical bonds play an important role for determining the preferred OR for the Ni/YSZ system, which will be discussed in the next sections in detail.

3.3 Atomic structure

In order to investigate the atomic structures at the Ni/YSZ(111) interface, multislice simulations were performed and the simulated images were compared with the experimental HRTEM images. For simplicity, a pure cubic zirconia was assumed, although the real system includes a certain amount of yttrium ions. For HRTEM image simulations, possible model structures were constructed for the Ni/YSZ(111) system. It should be noted, however, that the assumed YSZ lattice is composed of the Zr and O sublattices, and thus the terminated planes at the interfaces have to be taken into account. In the present case, O-terminated and Zr-terminated interfaces can be considered for the Ni/YSZ(111) system. For image simulation, defocus values and specimen thicknesses were varied systematically so that the simulated images are consistent with the HRTEM images.

Figure 4 shows model structures of (a) the O-terminated and (b) the Zr-terminated interfaces. In the simulated images displayed in Fig. 4(c) and (d), a defocus value of −26 nm and a specimen thickness of 4.5 nm were used, to reproduce the experimental HRTEM image in Fig. 1. Furthermore, a magnified HRTEM image of Fig. 1 is shown in Fig. 4(e) in order to make comparison with the simulated images. In the simulations, the interlayer distances were set to be 0.197 nm for the O-terminated model and 0.276 nm for the Zr-terminated model across the interface, which were energetically stable bond lengths for Ni-O and Ni-Zr, reported by Christensen and Carter using ab initio calculations.[5] As can be seen from Fig. 4(c) and (d), dark spots correspond to Ni, Zr and O columns in these imaging conditions. It can be seen that these two simulated images exhibit quite similar arrangements of both bright and dark spots at the interfaces, and are also consistent with the experimental image. It was, therefore, hard to determine which model is comparable with the actual Ni/YSZ(111) interface only by the HRTEM image simulations. For this reason, it is necessary to analyze the chemical bonding states at the interface.

3.4 Electronic structure

EELS is a powerful technique for investigating chemical bonding states in narrow regions such as grain boundaries and interfaces. This is because near edge structures of core-loss peaks in an EELS spectrum (electron energy-loss near-edge structure, or ELNES) reflect local structural and chemical environments of constituent atoms. To reveal the chemical bonding states of the Ni/YSZ interfaces, EELS spectra were measured in the vicinity of and at the interface by focusing electron beams onto specimens with a probe size less than 1.5 nm. All spectra were acquired for 10 s or less and accumulated just one time to decrease a readout noise.

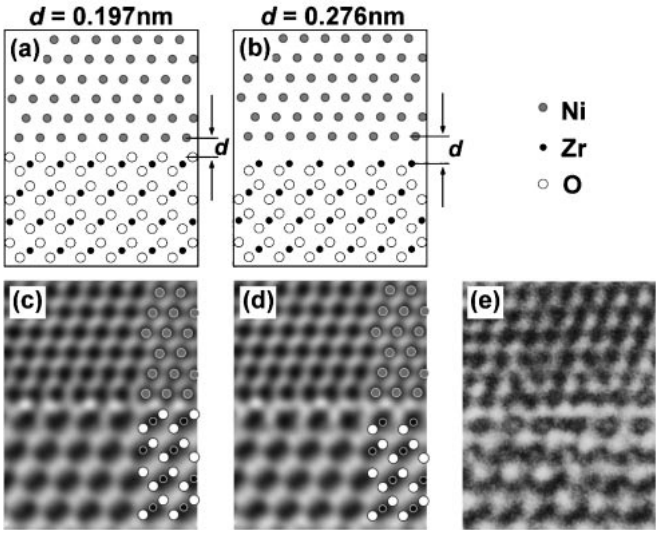

Fig. 4 Structural models of (a) the O-terminated and (b) the Zr-terminated Ni/YSZ(111) interfaces viewed along $[1\bar{1}0]_{\mathrm{Ni}} \parallel [1\bar{1}0]_{\mathrm{YSZ}}$. Gray, black and white circles represent Ni, Zr and O atoms, respectively. Simulated HRTEM images based on the models (a) and (b) at the defocus value of −26 nm and the specimen thickness of 4.5 nm are shown in (c) and (d), respectively. (e) Experimental HRTEM image.

Figure 5 shows O-K ELNES taken from (a) the interface and (b) the YSZ substrate. It can be seen that there are a number of differences in spectrum shape and peak energies between the two spectra. For example, the small shoulder A and peak E can be found only in the interface spectrum. The peaks B and D in the interface spectrum showed energy shifts from those in YSZ. In particular, it is obvious that the peak energy of D in (a) is shifted lower by 2 eV, as compared to that of D′ in YSZ. Furthermore, the additional feature C appeared, which is broader than the spectrum shape of YSZ in the same energy range. These differences in O-K ELNES indicate the interactions between Ni and O atoms at the interface.

In this case, the interface spectrum reflects Ni-O bonding features, and thus the spectrum was also compared with O-K ELNES of NiO reported by Kurata *et al.*[22] In fact, the energy of the features (A∼E) in the interface spectrum agreed well with that in NiO bulk, as shown in Fig. 5(a) and (c). However, the shapes of these peaks and shoulder in the interface spectrum are not always similar to those in the reference spectrum. It is noted that not only the oxygen atoms at the interface but also those in the YSZ substrate contribute to the obtained ELNES due to the finite size of the electron probe, although the electron beam used for EELS measurements is focused less than about 1.5 nm. Therefore, the O-K ELNES

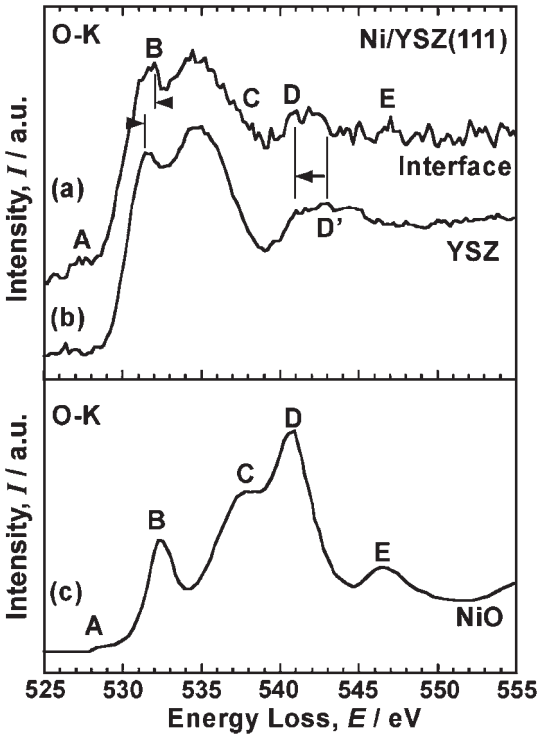

Fig. 5 O-K ELNES observed at (a) the interface and (b) the YSZ substrate in the Ni/YSZ system. Note that the energy of the peak D in (a) is lowered about 2 eV from the energy of the peak D′ in (b), and corresponds to the energy of the peak D in (c) reference O-K ELNES of NiO reported by Kurata *et al.*[22]

obtained from the interface (Fig. 5(a)) is considered to include information on a considerable amount of the oxygen atoms in the YSZ bulk region in addition to that of a small amount of the oxygen atoms located just at the interface. Thus, the NiO-like features in the interface spectrum are overlapped and weakened by the YSZ spectrum. However, as mentioned above, the energy of the peak D in the interface spectrum is lowered about 2 eV. This is strongly affected by a particular feature caused by the Ni-O interaction at the interface, which corresponds to the strong peak D in the NiO reference spectrum. Therefore, the NiO-like features (A∼E) in the O-K ELNES taken from the interface are the evidence that there are the Ni-O interactions across the interface. It can be said that the surface of YSZ(111) is terminated by an oxygen plane. In fact, the HRTEM image agreed well with the simulated HRTEM image based on the O-terminated model. This indicates that the Ni-O bonds play an important role for stabilizing the Ni/YSZ(111) interface.

Dickey *et al.* reported that Ni-Zr bonds predominate at Ni(111)/c-ZrO_2(001) interface (calcia-or yttria-stabilized zirconia) by Z-contrast imaging techniques and EELS analyses.[10] This is not consistent with our results of Ni-O bonding at the interface, although the ZrO_2 surface is different. One of the possible explanations for this discrepancy is the difference in the fabrication process. The above authors fabricated the Ni/c-ZrO_2 interface by reducing the NiO-ZrO_2 eutectics. In case of the reducing atmosphere, oxide ceramics are subjected to oxygen removals. It can be considered that the formation energy of Zr-terminated interfaces was lower than that of O-terminated interfaces in the reducing atmosphere due to lack of the oxygen atoms at the interface. Another reason for this discrepancy is the difference of the surface plane of ZrO_2. It is possible that not only the atomic and electronic structures but also the interfacial energy is different between Ni/ZrO_2(001) and Ni/ZrO_2(111) interfaces. According to recent theoretical studies, there are differences in the interfacial energies, which gives the actual stability of the each interface, between Ni(001)/ZrO_2(001)[9] and Ni(111)/ZrO_2(111)[5] interfaces, although the interface plane of Ni is different from each other. Furthermore, Beltrán *et al.* reported that both the Zr-terminated and the O-terminated interfaces are energetically favorable in the Ni(001)/ZrO_2(001) interface,[9] while Christensen and Carter reported that the O-terminated interface is energetically favorable in the Ni(111)/ZrO_2(111) interface,[5] which is consistent with our result. It can be expected that the chemical bonding states of the present Ni/YSZ(111) interface is similar to that reported by Christensen and Carter.

3.5 Effect of oxygen on-top nickel atoms

As mentioned in the section 3.2, there was a discrepancy between the experimental OR (I) and the most coherent OR (II). For CRLP calculation, only geometrical information such as lattice parameters was used. In order to take the chemical interaction into account, atomic configurations just at interface should be considered. Figure 6 shows the atomic configurations of the O-terminated Ni/YSZ(111) interface based on (a) the experimental OR (I) and (b) the most coherent OR (II), in which a Ni layer and an O layer at the interface are only shown. The black and white circles represent Ni and O atoms, respectively. The Ni atoms are located in the on-top, bridge and hollow sites of O atoms, as shown in Fig. 6(a), because of the difference in the lattice parameters between Ni and YSZ crystals. The Ni atoms are distributed isotropically on the YSZ(111) in the experimental OR due to the low index plane of Ni(111), while they are distributed anisotropically in the most coherent OR due to the high index plane of Ni(705). Thus, there is a difference in the number of on-top Ni atoms (overlapped Ni atoms) between the experimental OR and the most coherent OR. In order to evaluate this difference, overlapped atomic densities were calculated by a following method. If a distance "d" of the Ni-O in the two-dimensional projection (see Fig. 6(a)) is not larger than a critical distance "d_c", such O atoms are considered to have strong interactions with the Ni atoms at the on-top sites. A "d_c" value was defined as

$$d \leq d_c = aD \tag{3}$$

where "D" is a distance of O-O in the projection (See Fig. 6(a)), and "a" is an arbitrary constant. First of all, a circular cell, in which Ni and YSZ interface planes were expanded periodically, was used for the calculation of the overlapped atomic density. Since the cell size should be large enough so that the overlapped atomic density is independent of the cell size, it was set to 30 nm in diameter. Secondly, the overlapped atomic density was calculated by changing the "a" value. It was found that the overlapped atomic densities were proportional to the arbitrary constant "a", and yet relative atomic densities for the two interfaces studied here were also independent of the value of "a". Therefore, the arbitrary

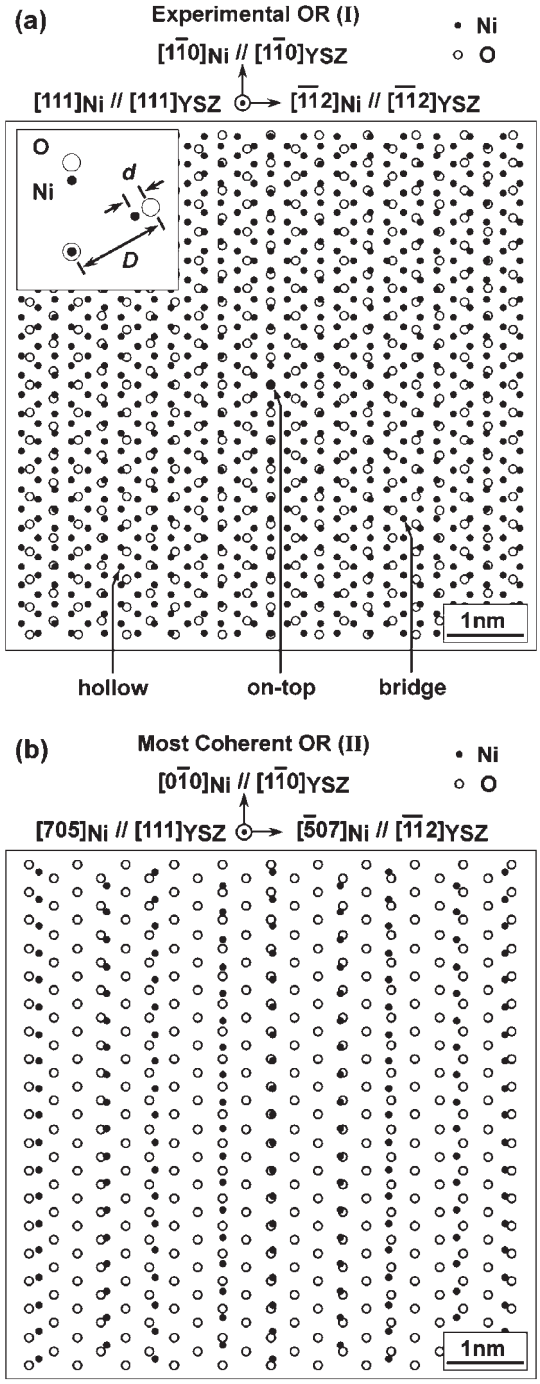

Fig. 6 Atomic configurations of the Ni/YSZ(111) interface based on (a) the experimental OR (I) and (b) the most coherent OR (II), in which the Ni layer and the O layer closest to the interface are only shown. Black and white circles represent Ni and O atoms, respectively. Note that Ni atoms are distributed isotropically on the YSZ(111) in (a) the experimental OR, while they are distributed anisotropically in (b) the most coherent OR. Distances of Ni-O and O-O defined by eq. (3) are shown in the inset.

constant "a" was set to 0.15 for the present calculations. From these calculations, it was found that the overlapped atomic densities in the experimental OR and the most coherent OR were $1.58\,\mathrm{nm}^{-2}$ and $0.16\,\mathrm{nm}^{-2}$, respectively. That is, the experimental OR had ten times larger overlapped atomic density than the most coherent OR. This indicates that the on-top Ni atoms (overlapped Ni atoms) on the O atoms influence the stability of the Ni/YSZ(111) interface. The experimental OR tends to have larger overlapped atomic density than the most coherent OR obtained by CRLP calculation. In fact, it was found in our previous study that this tendency is also true for $Cu/Al_2O_3(0001)$ and $(11\bar{2}0)$ interfaces.[16,17]

Hernández and Sanz reported the interlayer distances between Cu and O layers in O-terminated $Cu/Al_2O_3(0001)$ interface using ab initio calculations.[23] Calculating the Cu-O bond length based on their report, the Cu-O bond lengths of the on-top and hollow O sites resulted in 0.208 nm and 0.252 nm, respectively, which indicates that Cu-O bonds of the on-top O sites were likely to be shorter than those of the hollow O sites. In fact, there is a similar tendency in the Cu/MgO(111) system.[24] By taking account of the image force potential model,[25] the shorter metal-oxygen (M-O) bond length results in stronger interactions between metal and oxygen atoms, while the longer M-O bond length results in weaker interactions. It is, therefore, likely that the on-top M-O bonds stabilize the interface. The present result that the most coherent OR is not formed in the Ni/YSZ(111) interface is attributed to the fact that the observed OR has larger overlapped atomic density (on-top Ni-O bonds) than the most coherent ORs. From the present analysis, it can be concluded that the interfaces are likely to be formed so as to make the larger numbers of the on-top Ni-O bonds across the interfaces. Therefore, the number of the on-top M-O bonds is one of the critical factors that can determine the stability of the Ni/YSZ interfaces as well as the Cu/Al_2O_3 system.[16,17]

4. Conclusions

In order to understand the atomic and electronic structures in the Ni/YSZ(111) interface, HRTEM observations, EELS measurements and geometrical analyses were performed. The results obtained in this study are summarized as follows.

1. The (111) plane of Ni metal was epitaxially oriented to the YSZ(111) surface, and the following cube-on-cube OR was obtained: $(111)_{Ni} \parallel (111)_{YSZ}$, $[1\bar{1}0]_{Ni} \parallel [1\bar{1}0]_{YSZ}$.
2. The most coherent OR predicted by CRLP calculation was the following OR: $(705)_{Ni} \parallel (111)_{YSZ}$, $[0\bar{1}0]_{Ni} \parallel [1\bar{1}0]_{YSZ}$. However, this most coherent OR was not consistent with the experimental OR observed in the Ni/YSZ(111) interface.
3. The NiO-like features were observed in the ELNES obtained from the interface, whereas they were not observed in the ELNES obtained from the YSZ substrate, which indicate that there are interactions between Ni and O atoms across the interface.
4. Considering the atomic configurations of the O-terminated interfaces, it was found that the experimental OR had larger overlapped Ni atomic density at the interface than the most coherent ORs. It can be concluded that the interfaces are likely to be formed so as to make the larger numbers of the on-top Ni-O bonds across the Ni/YSZ interfaces. It is, therefore, likely that the number of the on-top M-O bonds is one of the critical factors that can determine the stability of the metal/oxide interfaces.

Acknowledgements

The authors wish to thank Dr. T. Mizoguchi, for fruitful discussions. This work was performed as a part of Nanostructure Coating Project carried out by New Energy and Industrial Technology Development Organization. The present research is also supported in part by a Grant for 21st Century COE Program "Human-Friendly Materials based on Chemistry" from the Ministry of Education, Culture, Sports, Science, and Technology of Japan.

REFERENCES

1) P. K. Wright and A. G. Evans: Curr. Opin. Solid State Mater. Sci. **4** (1999) 255–265.
2) A. G. Evans, D. R. Mumm, J. W. Hutchinson, G. H. Meier and F. S. Pettit: Prog. Mater. Sci. **46** (2001) 505–553.
3) N. Q. Minh: J. Am. Ceram. Soc. **76** (1993) 563–588.
4) T. Fukui, S. Ohara and K. Mukai: Electrochem. Solid State Lett. **1** (1998) 120–122.
5) A. Christensen and E. A. Carter: J. Chem. Phys. **114** (2001) 5816–5831.
6) X. Han, Y. Zhang, S. Gong and H. Xu: Key Eng. Mater. **224–226** (2002) 355–358.
7) X. Han, Y. Zhang and H. Xu: Chem. Phys. Lett. **378** (2003) 269–272.
8) J. I. Beltrán, S. Gallego, J. Cerdá and M. C. Muñoz: J. Eur. Cera. Soc. **23** (2003) 2737–2740.
9) J. I. Beltrán, S. Gallego, J. Cerdá, J. S. Moya and M. C. Muñoz: Phys. Rev. B. **68** (2003) 075401.
10) E. C. Dickey, X. Fan and S. J. Pennycook: Acta Mater. **47** (1999) 4061–4068.
11) E. C. Dickey, Y. M. Bagiyono, G. D. Lian, S. B. Sinnott and T. Wagner: Thin Solid Films. **372** (2000) 37–44.
12) J. M. Rigsbee and H. I. Aaronson: Acta Metall. **27** (1979) 351–363.
13) R. W. Balluffi, A. Brokman and A. H. King: Acta Metall. **30** (1982) 1453–1470.
14) Y. Ikuhara and P. Pirouz: Mater. Sci. Forum. **207–209** (1996) 121–124.
15) R. Kilaas: the 49th EMSA Meeting, ed. by G.W. Bailey, (San Francisco Press, San Francisco, 1991) pp. 528–529.
16) T. Sasaki, K. Matsunaga, H. Ohta, H. Hosono, T. Yamamoto and Y. Ikuhara: J. Soc. Mater. Sci. Japan. **52** (2003) 555–559.
17) T. Sasaki, K. Matsunaga, H. Ohta, H. Hosono, T. Yamamoto and Y. Ikuhara: Sci. Technol. Adv. Mater. **4** (2003) 575–584.
18) Y. Ikuhara and P. Pirouz: Ultramicroscopy **52** (1993) 421–428.
19) Y. Ikuhara, P. Pirouz, A. H. Heuer, S. Yadavallis and C. P. Flynn: Philos. Mag. A. **70** (1994) 75–97.
20) Y. Ikuhara and P. Pirouz: Micros. Res. Techniq. **40** (1998) 206–241.
21) Y. Ikuhara: J. Ceram. Soc. JPN. **109** (2001) S110–S120.
22) H. Kurata, E. Lefèvre, C. Colliex and R. Brydson: Phys. Rev. B. **47** (1993) 13763–13768.
23) N. C. Hernández and J. F. Sanz: J. Phys. Chem. B **106** (2002) 11495–11500.
24) R. Benedek, D. N. Seidman, M. Minkoff, L. H. Yang and A. Alavi: Phys. Rev. B **60** (1999) 16094–16102.
25) P. W. Tasker and A. M. Stoneham: J. Chimie. Phys. **84** (1987) 149–155.